Molecular Therapy
Nucleic Acids
Original Article

Terminal bridging of siRNA duplex at the ribose 2′ position controls strand bias and target sequence preference

Atsushi Shibata,[1] Hisao Shirohzu,[1,2] Yusuke Iwakami,[1] Tomoaki Abe,[1] Chisato Emura,[1] Eriko Aoki,[1] and Tadaaki Ohgi[1]

[1]Division of R&D, Bonac Corporation, 1488-4 Aikawa, Kurume, Fukuoka 839-0861, Japan; [2]Fukuoka Center for Disease Control and Prevention, Kurume, Fukuoka, Japan

Small interfering RNA (siRNA) and short hairpin RNA (shRNA) are widely used as RNA interference (RNAi) reagents. Recently, truncated shRNAs that trigger RNAi in a Dicer-independent manner have been developed. We generated a novel class of RNAi reagent, designated enforced strand bias (ESB) RNA, in which an siRNA duplex was chemically bridged between the 3′ terminal overhang region of the guide strand and the 5′ terminal nucleotide of the passenger strand. ESB RNA, which is chemically bridged at the 2′ positions of ribose (2′-2′ ESB RNA), functions in a Dicer-independent manner and was highly effective at triggering RNAi without the passenger strand-derived off-target effect. In addition, the 2′-2′ ESB RNA exhibited a unique target sequence preference that differs from siRNA and silenced target sequences that could not be effectively suppressed by siRNA. Our results indicate that ESB RNA has the potential to be an effective RNAi reagent even when the target sequence is not suitable for siRNA.

INTRODUCTION

RNA interference (RNAi) is a post-transcriptional gene silencing event that is widely conserved in eukaryotes.[1,2] RNAi reagents, such as small interfering RNAs (siRNAs) or short hairpin RNAs (shRNAs), have been routinely used for the analysis of gene function,[3,4] and a number of clinical trials are ongoing to evaluate RNAi-based drugs.[5–7] In the cytoplasm, siRNA is incorporated into a protein complex called the RNA-induced silencing complex (RISC), which plays a central role in the cleavage of the target mRNA. The two strands that comprise siRNA are not equivalent in the RISC because of a difference in their terminal thermodynamic stabilities.[8] The strand with a higher free energy at its 5′ terminus is selectively retained by the RISC and acts as a guide strand, whereas the other strand, known as the passenger strand, is ejected from the RISC (so-called strand bias).[9] This antisense strand-selective bias triggers target gene suppression; however, sense strand-selective strand bias results in off-target effects. Therefore, siRNA design rules include criteria that address the thermodynamic stability of siRNA termini so that the 5′ end of the antisense strand is less stable compared with that of the sense strand.[10–12] The guide strand in the RISC is captured by the Ago2 protein, which has target cleavage activity.[13] Although terminal thermodynamic stability is one of the key determinants of RISC uptake of siRNAs in human cells, recent studies have shown that strand bias is not solely determined by asymmetric terminal stability.[14,15] The MID and PAZ domains of the Ago2 protein bind to the guide strand through the phosphate group at the 5′ terminus and to the hydroxy group at the 3′ terminus and base of the guide strand, respectively.[16–19]

Ordinary shRNAs are processed by the Dicer endoribonuclease to produce siRNAs; however, several groups have reported a class of truncated shRNAs with stem lengths of 19 bp or less that can trigger RNAi in a Dicer-independent manner. These truncated shRNAs show reduced passenger strand-derived off-target effects[20–23] and are incorporated into the RISC while retaining the loop structure.[21,22] Therefore, the reduced passenger strand activities may result from the protection of the 5′ end of the passenger strand by the nucleotide loop. However, the loop structure stabilizes the hybridization of RNA duplex around the loop side, and the opposite terminus becomes relatively looser. This thermodynamic stabilization of the loop side in truncated shRNAs may also be the basis for guide strand-selective RISC incorporation.

In this study, we generated two types of siRNAs in which the duplexes are chemically bridged. We discovered that the chemical bridging of the siRNA duplex controls strand bias independently of the protection at the 5′ end of the passenger strand. Therefore, we designated this strong, biased guide strand selection resulting from chemical bridging between the guide and passenger strands as “enforced strand bias (ESB),” and the chemically bridged siRNAs as “ESB RNAs.” We found that ESB RNA has a unique target sequence preference, which is different from siRNA, and it suppresses target sequences that may not be possible with siRNAs.

Received 4 November 2022; accepted 14 April 2023;
https://doi.org/10.1016/j.omtn.2023.04.013.

Correspondence: Atsushi Shibata, Division of R&D, Bonac Corporation, 1488-4 Aikawa, Kurume, Fukuoka 839-0861, Japan.
E-mail: atsushi.shibata@bonac.co.jp

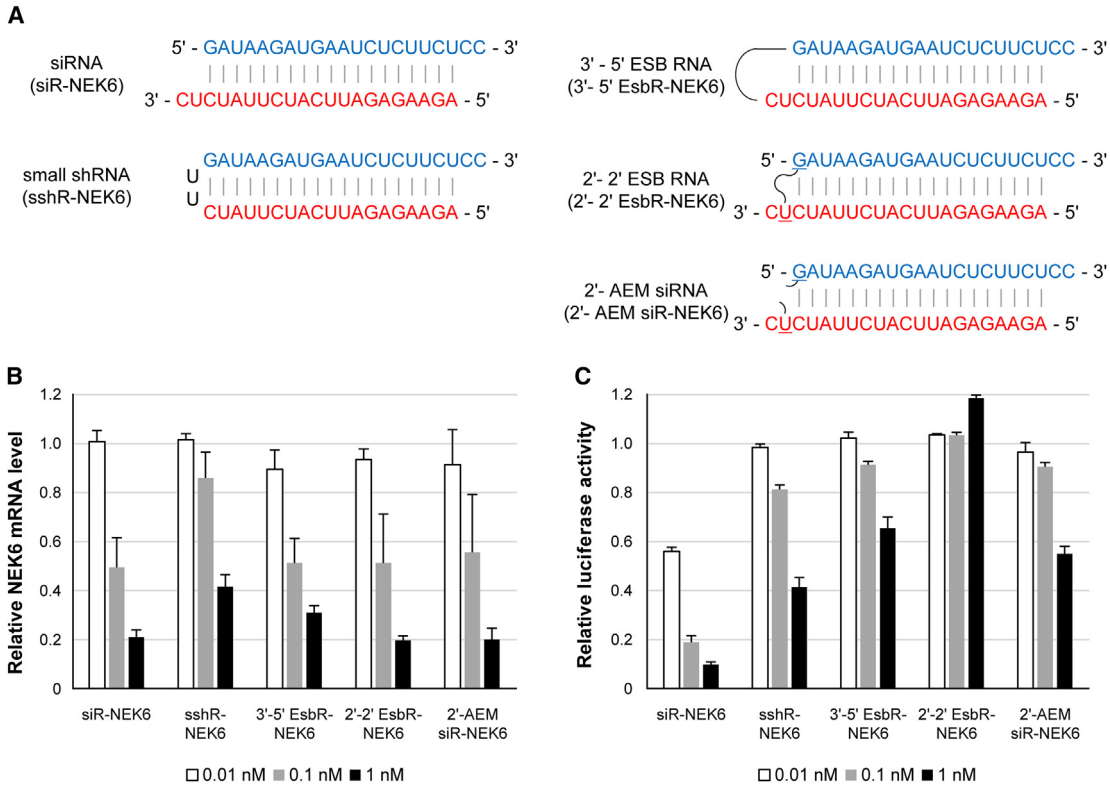

Figure 1. Comparison of the structures and silencing efficacies of siRNA and its bridged derivatives

(A) The siRNA duplex targeting human *NEK6* and derivatives. The siRNA duplex was bridged with a dinucleotide linker using a small shRNA at the 3′ end of the guide strand and the 5′ end of passenger strand (sshR-NEK6). The siRNA duplexes were chemically bridged with 1,6-bis (hexylamide) hexane at the 3′ position of the 3′ terminal nucleotide ribose of the guide strand and the 5′ position of the 5′ terminal nucleotide ribose of the passenger strand (3′-5′-type ESB RNA) or at the ribose 2′ position of the second nucleotide from the 3′ end of the guide strand and the ribose 2′ position of the 5′ terminal nucleotide of the passenger strand (2′-2′ ESB RNA). The blue letters represent the passenger strand, and red letters represent the guide strand. The 2′-AEM-modified nucleotides are indicated as underlined letters. Black curved lines are the schematic representation of non-nucleotide linkers. Gray vertical lines indicate hybridization of two strands through hydrogen bonds. See also Figure S1. (B and C) The guide strand activity was measured as target mRNA levels by qRT-PCR (B), and the passenger strand activity was measured as reporter protein activity using a luciferase assay (C). Bars represent the means ± standard deviation (n = 3).

RESULTS

Synthesis of ESB RNAs

To bridge the guide and passenger strands of siRNA with an alkyl chain at the 2′ position of the ribose in the oligonucleotide, we initially developed trifluoroacetylaminoethoxymethyl (AEM) amidites (Figure S1A). The AEM amidites were incorporated at the second nucleotide position from the 3′ end of the guide strand and the 5′ terminal position of the passenger strand of the siRNA duplex during synthesis. The synthesized guide and passenger strands harboring the AEM modification were annealed and bridged with bis(sulfosuccinimidyl)suberate disodium salt (Figure S1A) between the AEM groups at the ribose 2′ position. The resulting 2′-2′ ESB RNA (Figures 1A and S1B) was one of the optimized structures of ESB RNA. To produce 3′-5′ ESB RNA, the synthesized guide and passenger strands containing the aminohexyl modification were annealed and bridged under the same conditions as the 2′-2′ ESB RNA (Figure S1C).

ESB RNA exhibits gene silencing activity and eliminates passenger strand activity

To determine whether the protection of the 5′ end of the passenger strand is essential for the selective strand bias of the guide strand, siRNA, small shRNA (sshRNA),[21] and two ESB RNAs (3′-5′ type and 2′-2′ type) were designed to target the human *NEK6* mRNA (Figure 1A). These siRNA and their derivatives were transfected into cultured cells. Subsequently, reverse transcription followed by quantitative polymerase chain reaction (qRT-PCR) and a luciferase assay were performed to measure the silencing efficiency of the guide and passenger strands. qRT-PCR revealed that the silencing activities of the 2′-2′ ESB RNA and the 2′-AEM-modified siRNA were comparable with that of siRNA, thus the 2′-AEM modification and chemical bridging used here did not appear to inhibit RISC incorporation of the guide strand (Figure 1B). The sshRNA and the 3′-5′ ESB RNA exhibited a slightly weaker silencing efficacy compared with siRNA, suggesting that the protection of the 3′ end of the guide strand may negatively affect the RNAi pathway

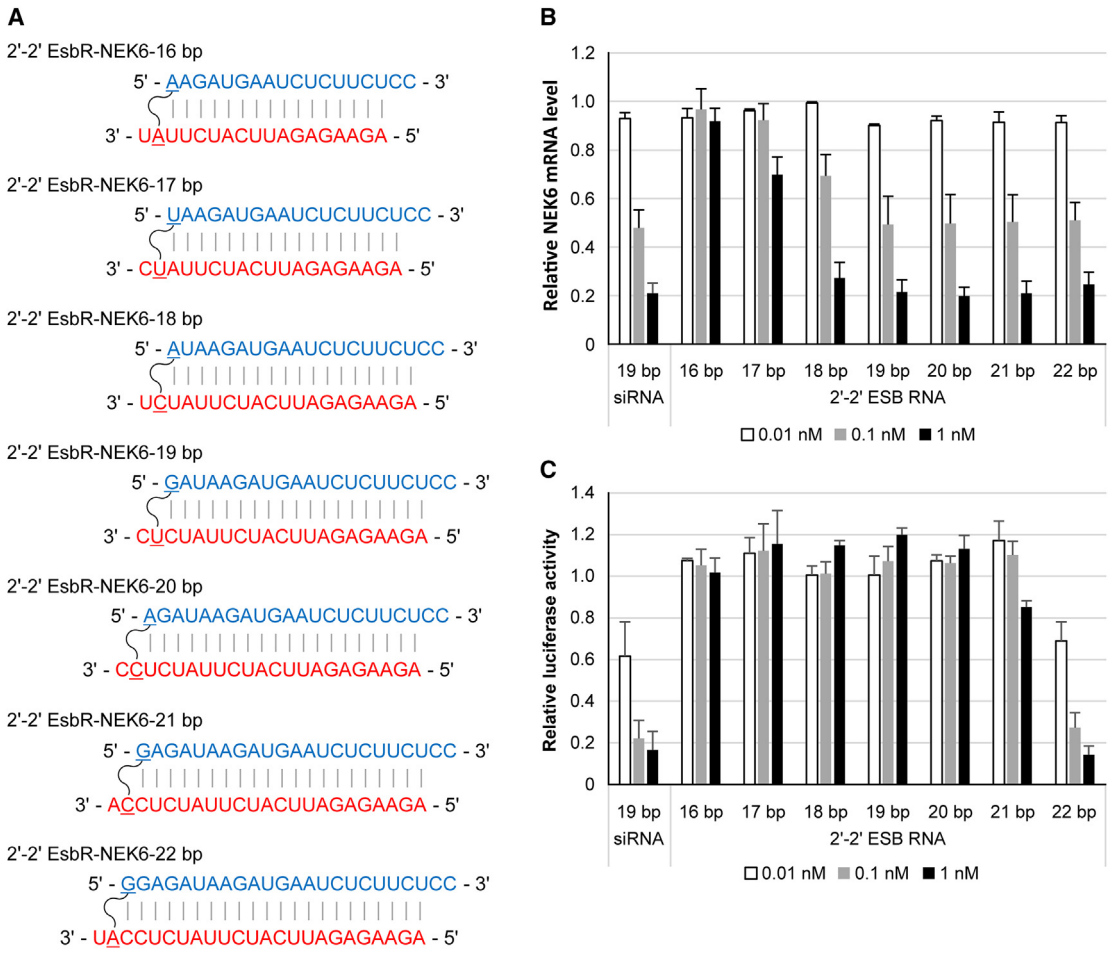

Figure 2. Stem length dependency of 2′-2′ ESB RNAs targeting human *NEK6*

(A) Length variations of the ESB RNA targeting human *NEK6*. The blue letters represent the passenger strand, and red letters represent the guide strand. The bridged nucleotides are underlined. (B and C) The guide strand activity was measured as the target mRNA levels by qRT-PCR (B), and the passenger strand activity was measured as reporter activity using a luciferase assay (C). Bars represent the means ± standard deviation (n = 3). See also Figures S2 and S3.

(Figure 1B). The luciferase assay indicated that the passenger strand activity was significantly inhibited in the sshRNA, ESB RNAs, and 2′-modified siRNA compared with the siRNA that exhibited a strong silencing effect by the passenger strand (Figure 1C). Of note, the passenger strand activity of the 2′-2′ ESB RNA was eliminated, whereas the passenger strand activities of sshRNA, 3′-5′ ESB RNA, and 2′-AEM-modified siRNA were weak but still evident (Figure 1C). These results suggest that protection of the guide strand 3′ end is not essential to inactivate the passenger strand and not sufficient to eliminate passenger strand activity. Although the 2′-AEM modification itself had the effect of attenuating passenger strand activity, cross-link formation was essential for the disappearance of passenger strand activity. Our results indicate that only 2′-2′ ESB RNA exhibits perfect guide strand-selective RISC incorporation, with the highest guide strand silencing efficiency and no passenger strand activity.

Evaluation of the stem length of 2′-2′ ESB RNA required for guide strand-selective RISC incorporation

To confirm the stem length of 2′-2′ ESB RNA that triggers gene silencing without passenger strand activity, the *NEK6*-targeted 2′-2′ ESB RNAs of 16–22 bp in length were designed and synthesized as shown in Figure 2A. Then, qRT-PCR was performed on these ESB RNAs 24 h after transfection (Figure 2B). The results indicated that ESB RNAs longer than 18 bp suppressed target gene expression similar to siRNA, indicating RISC incorporation of the guide strand. The 17 bp ESB RNA exhibited reduced suppression efficiency for the guide strand, and the silencing activity was eliminated in the 16 bp ESB RNA, indicating a defect in RISC incorporation for the ESB RNAs of less than 18 bp. In addition, the silencing efficacy of the passenger strand was measured by luciferase assay to confirm whether the 2′-2′ bridging could inhibit RISC incorporation of the passenger strand (Figure 2C). The loss or significant reduction of silencing

activity of the passenger strand was observed when the siRNA lengths were 16–21 bp. A significant silencing activity of the passenger strand was observed only when the ESB RNA was 22 bp, with a slight trend toward dose-dependent passenger strand activity at 21 bp. These results suggest that 2′-2′ ESB RNA duplexes longer than 21 bp may be processed by Dicer, which results in the removal of the chemical bridges. To confirm Dicer dependency of the 2′-2′ ESB RNAs, the *NEK6*-targeting 2′-2′ ESB RNAs of 18–22 bp length were transfected into Dicer-knockout H1299 cells. The silencing activities of the guide strand were measured by qRT-PCR (Figure S2A) and were similar to the results obtained with Dicer-expressing H1299 cells (Figure 2B). This indicates that the silencing activity of the 2′-2′ ESB RNAs guide strand was Dicer independent. The luciferase assay measuring passenger strand activity revealed the elimination of the passenger strand activities of 21–22 bp ESB RNAs under Dicer-deficient conditions (Figure S2B). Therefore, 2′-2′ ESB RNAs longer than 21 bp may be a substrate for Dicer.

To confirm the applicability of 2′-2′ ESB RNA to other targets, we synthesized 18–21 bp 2′-2′ ESB RNAs targeting human *HPRT1* mRNA (Figure S3A) and introduced them into cultured cells. The results of qRT-PCR measuring the expression of *HPRT1* mRNA indicated that the ESB RNAs exhibited compatible silencing efficiency with the positive control siRNA, which is consistent with the results of *NEK6* targeting described above (Figure S3B). However, the luciferase assay indicated that the passenger strand of the 21 bp ESB RNA was still active, whereas the off-target effect was weakened, which was different from that observed for *NEK6* targeting (Figure S3C). Thus, the range in length for ESB RNAs that can eliminate passenger strand activity while maintaining silencing activity of the guide strand comparable with that of siRNA was 18–20 bp. Among the 18–20 bp ESB RNAs, the 18 bp ESB RNAs had slightly lower silencing efficiency, although no statistical significance was evident. Therefore, the 19 or 20 bp ESB RNAs were used in subsequent experiments.

Target sequence preference of 2′-2′ ESB RNA is partially different from that of siRNA

The almost perfect guide strand-selective RISC incorporation observed with ESB RNAs prompted us to hypothesize that the 19 or 20 bp length 2′-2′ ESB RNAs could suppress any sequence, even those that cannot be suppressed by siRNAs. To evaluate the silencing efficiency of 2′-2′ ESB RNAs against various target sequences, 30 ESB RNAs were designed to target different sites of the human *GAPDH* mRNA coding region (Table S1). The target sequences were selected to have less off-target effects by referring to the off-target prediction score obtained using siSPOTR[24] (Table S1). Each target site was confirmed whether they could be selected as an siRNA target site in the siRNA design tool siDirect[25] (Table S1; Figure 3A). As the result, seven sites (GAP-02, -04, -05, -14, -15, -16, and -17) were selected when the *GAPDH* mRNA sequence was applied to siDirect. In contrast, eight target sites (GAP-06, -07, -12, -13, -18, -24, -25, and -28) were selected when siRNAs were designed based on the complementary sequence (antisense) of the human *GAPDH* mRNA; therefore, the siRNAs targeting these sites were expected to be less effective. The other 15 target sites (GAP-01, -03, -08, -09, -10, -11, -19, -20, -21, -22, -23, -26, -27, -29, and -30) were not selected in either the mRNA-based or the antisense-based siRNA design.

The siRNAs and 2′-2′ ESB RNAs targeting these sequences (Table S1) were transfected into H1299 cells. As the result of qRT-PCR analysis, siRNAs found in the mRNA-based target sites suppressed *GAPDH* expression by at least 80%, except for one siRNA targeting GAP-17 (less than 60% suppression). Interestingly, six of eight siRNAs found in the antisense-based target sites exhibited >80% suppression, even though their guide strand selection was predicted to be biased against the passenger strand. Most of the other siRNAs that were not selected in the siRNA design tool showed suppression of 80% or more, except for two siRNAs targeting GAP-08 and -19 (approximately 16% and 34% suppression, respectively).

The suppression efficiencies of these siRNAs were compared with the 2′-2′ ESB RNAs with identical sequences (Figure 3A). More than a half of these 2′-2′ ESB RNAs resulted in similar suppression efficacies compared with the identical siRNAs. It is noteworthy that enhanced silencing efficiencies were observed for the 2′-2′ ESB RNAs targeting GAP-07, -08, -10, -13, -18, and -25, whereas the 2′-2′ ESB RNAs targeting GAP-05, -14, -15, -17, -23, and -30 exhibited reduced suppression compared with their corresponding siRNAs. These results indicate that bridge formation between the sense and guide strands partially alters target sequence preference of the siRNAs. Interestingly, enhanced silencing was not observed with the ESB RNAs that were selected based on the target mRNA, and conversely, reduced silencing was not observed with ESB RNAs selected based on the antisense sequence.

To confirm whether ESB RNA exhibited enhanced silencing when the target sequences were not suppressed by siRNA, six target sequences were selected from the results of siRNA designs based on the antisense sequence of human *NEK6* mRNA (Table S2). The corresponding siRNAs and ESB RNAs (Table S2) were transfected into H1299 cells prior to RNA extraction and qRT-PCR. As expected, five siRNAs exhibited moderate or weak (less than 60%) silencing efficacy, except siR-NEK05 (approximately 79% suppression), as shown in Figure 3B. Surprisingly, higher silencing efficacies were observed for ESB RNAs compared with the identical siRNAs for all five target sites that were suppressed less than 60% by the siRNAs (Figure 3B). These data suggest that ESB RNAs have the potential to suppress target sequences that are not suppressed by siRNAs.

ESB RNA, but not siRNA, suppresses *EML4/ALK* fusion transcripts

In case the targetable sequence is limited, such as the junction of a fusion gene transcript, it may be difficult to design effective siRNAs. The fusion between echinoderm microtubule-associated protein-like 4 (*EML4*) and anaplastic lymphoma kinase (*ALK*) is an oncogenic driver that is often found in non-small cell lung cancer (NSCLC). There are several fusion variations of the *EML4-ALK* fusion gene, and variant 3 (*EML4* exon 6 fused to *ALK* exon 20) is

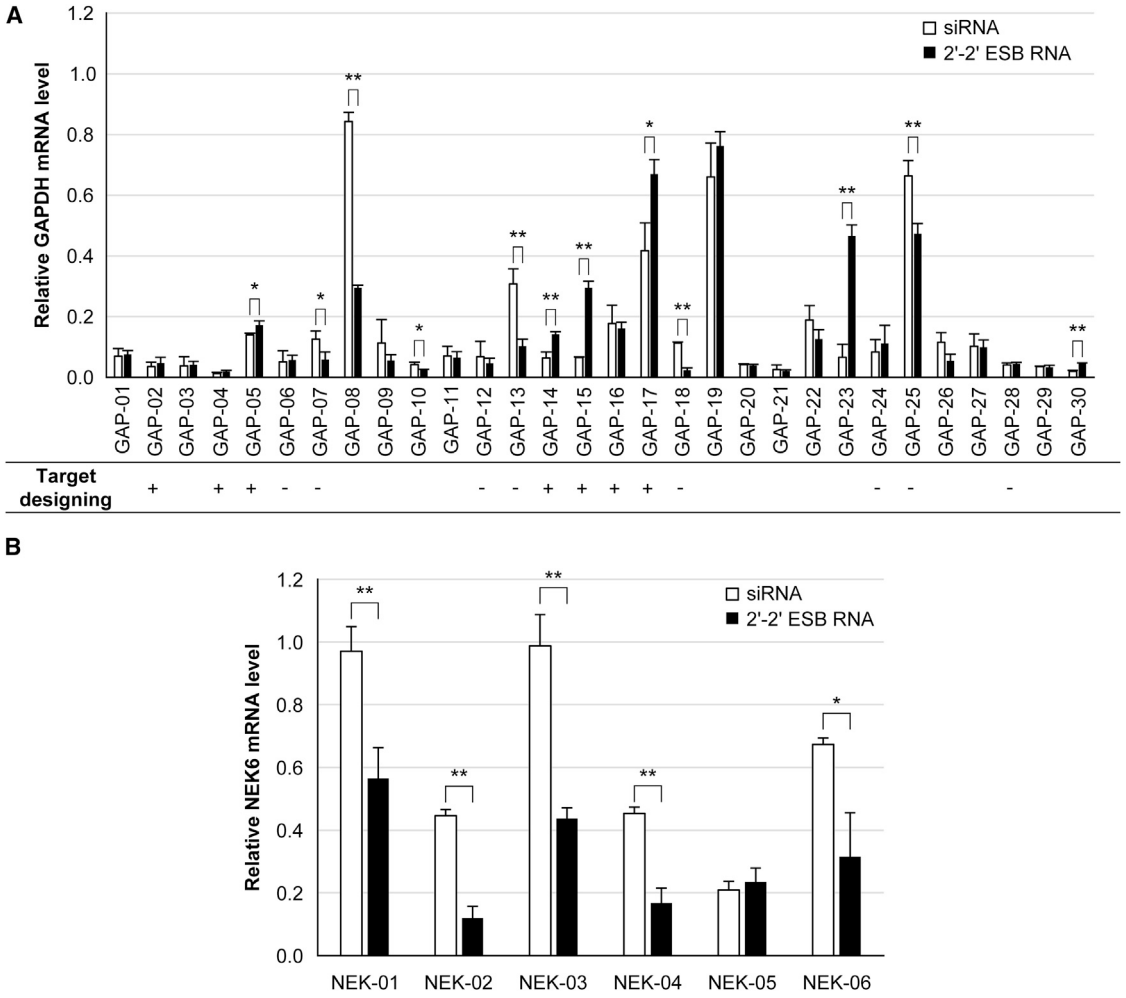

Figure 3. Comparison of silencing potency of siRNA and 2′-2′ ESB RNA

The siRNA or 2′-2′ ESB RNA was transfected at a final concentration of 10 nM into H1299 cells. The target mRNA levels were measured by qRT-PCR. (A) Guide strand activities of the human *GAPDH*-targeted siRNAs and ESB RNAs. The target sequences were selected independently by siRNA design tools, except for off-target prediction by siSPOTR. The results of siRNA target design based on the human *GAPDH* mRNA or its complementary sequence are shown below the target site numbers as "+" (selected for mRNA-based design) or "−" (selected for antisense-based design), respectively. The target sequences without "+" or "−" were not selected in each case. See also Table S1. (B) The guide strand activities of the siRNAs and 2′-2′ ESB RNAs targeting inappropriate sites for siRNA in the human *NEK6* mRNA. The target sequences were selected based on the antisense sequence of the NEK6 mRNA using the siRNA design tool siDirect and were not considered suitable for siRNA (see also Table S2). White bars and black bars are the relative target gene expression levels following transfection of siRNA or 2′-2′ ESB RNA, respectively. Bars represent the means ± standard deviation (n = 3). *p < 0.05 and **p < 0.01 in a Student's t test.

the second major type in *EML4-ALK*-driven NSCLC.[26,27] The sequence around the junction appears to be a poor target for siRNAs because a GC stretch is located downstream of the fusion point (Figure 4A). To determine whether ESB RNAs can overcome this limitation, we designed and synthesized siRNAs and ESB RNAs targeting the *EML4-ALK* variant 3 transcript (Figure 4B). Because the variant 3 *EML4-ALK* fusion gene produces two transcript variants, 3a and 3b, resulting from alternative splicing,[28] we constructed luciferase reporter plasmids carrying the junction sequences corresponding to *EML4-ALK* variants 3a and 3b to distinguish the silencing effects against these mRNAs independently. Using a luciferase assay, the silencing efficiency for variant 3a of all the 2′-2′ ESB RNAs targeting the variant 3 *EML4-ALK* fusion gene was greater than 70%, whereas that of the siRNAs was less than 60% (Figure 4C). The 2′-2′ ESB RNAs targeting EA3a-1, -2, and -3 suppressed luciferase activity by 70%, 89%, and 91%, respectively, and the siRNAs targeting EA3a-1, -2, and -3 suppressed luciferase activity by 56%, 52%, and 34%, respectively. Thus, the 2′-2′ ESB RNAs were more effective compared with siRNAs, although the silencing efficiency against the variant 3b was lower than that of the variant 3a for both 2′-2′ ESB RNAs and siRNAs, which was likely the result of mismatches around the guide strand 3′ ends (Figure 4D). Of note, EsbR-EA3a-03

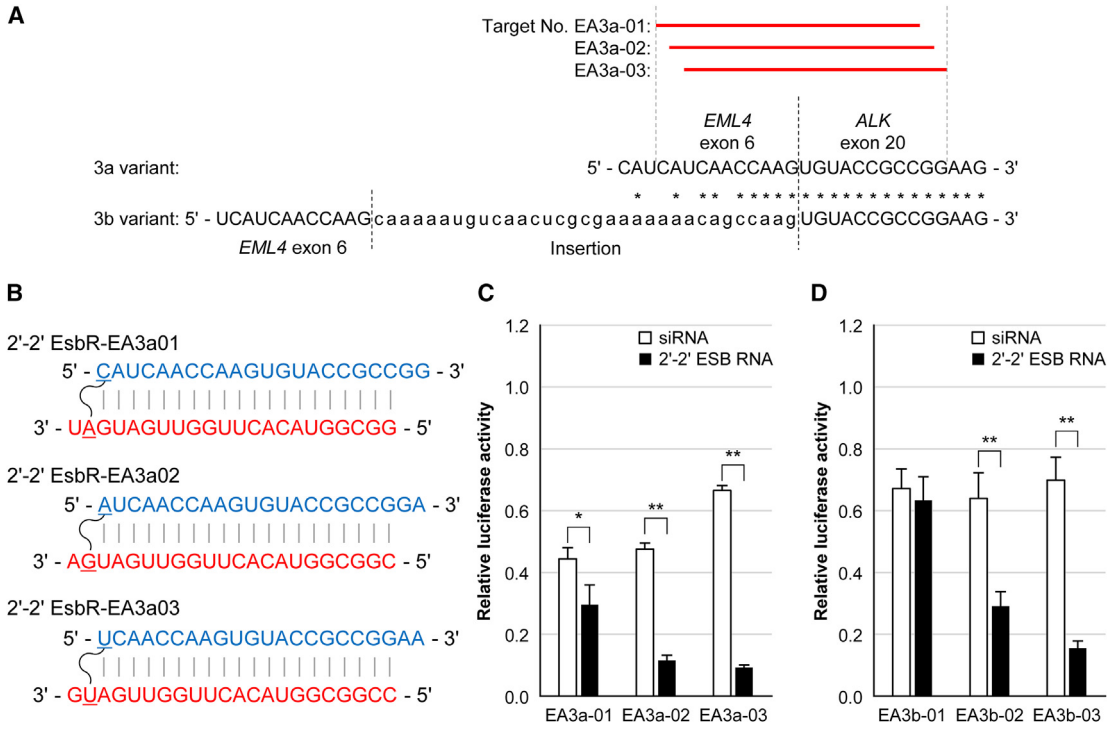

Figure 4. Knockdown of the *EML4-ALK* fusion transcripts by siRNAs or 2′-2′ ESB RNAs

(A) The schematic representation of the *EML4-ALK* fusion transcript variants 3a and 3b. The target sites, EA3a-01, -02, and -03 are indicated as red lines. (B) The sequences of the ESB RNAs targeting the *EML4-ALK* variant 3 transcripts. (C and D) The siRNA or 2′-2′ ESB RNA was transfected at a final concentration of 10 nM into HCT116 cells previously transfected with a luciferase expression vector. A luciferase assay was used to measure the knockdown efficacies of siRNAs and ESB RNAs against *EML4-ALK* fusion transcript variants 3a (C) and 3b (D). Bars represent the means ± standard deviation (n = 3).

suppressed approximately 85% of the variant 3b expression, whereas the suppression by siRNA at the same site (siR-EA3a-03) was 30%. Taken together, we demonstrated that only EsbR-EA3a-03 was sufficiently potent to suppress both mRNA variants 3a and 3b, whereas none of the siRNAs could simultaneously suppress both transcripts.

DISCUSSION

It has been demonstrated that protection of the 5′ end of the passenger strand with a short nucleotide loop in truncated shRNAs can prevent RISC incorporation of the guide strand.[20–22] Off-target effects derived from the passenger strand were also significantly reduced. Siolas et al. suggested that the nucleotide loop structure of these truncated shRNAs may be cleaved by endogenous RNase.[20] Because loop cleavage results in the exposure of the 5′ terminal phosphate group of the passenger strand, it may cause the partial off-target effects that result from the passenger strand. Our results in Figure 1C suggest that sshRNA cannot inactivate the passenger strand completely. It has also been reported that siRNAs with 5′ end protection through chemical modifications exhibit a reduced, but slight, suppression effect.[29] Therefore, covering the passenger strand 5′ end may not alone be sufficient to eliminate passenger strand activity. The 3′-5′ ESB RNA also exhibited weakened passenger strand activity even though the 5′ end of the passenger strand was chemically modified and cross-linked to the 3′ end of guide strand. This supports insufficient strand bias control by protecting the 5′ end of the passenger strand. To our knowledge, this 2′-2′ ESB RNA is the first example of chemical bridging at specific positions of the siRNA duplex. We demonstrated that 2′-2′ ESB RNA, in which the guide strand and passenger strand of siRNA are bridged at the 2′ positions of ribose by a non-nucleotide linker, can almost completely inhibit passenger strand RISC incorporation, even though the 5′ end of the passenger strand is not protected. Therefore, the mechanisms for eliminating guide strand-selective RISC incorporation by ESB RNA may be different from chemically modified siRNAs or truncated shRNAs. Because bridging at the terminal region of double-stranded RNA increases the thermodynamic stability of the bridged end, it is expected that bridging the 3′ end of the guide strand strengthens hybridization at the 5′ end of the passenger strand. The 5′ end of the guide strand would become relatively looser, and guide strand-selective RISC incorporation occurs. Because incorporation of AEM-modified nucleotides into siRNA itself does not eliminate passenger strand activity, chemical bridging appeared to be more important for guide strand selection than steric hindrance of the AGO protein interaction by the 2′-AEM modification. Importantly, slight attenuation of silencing efficiency by the guide strand was observed in sshRNA and 3′-5′ ESB RNA, whereas it was comparable with 2′-2′ ESB RNA and 2′-AEM siRNA. This may result from the availability of the 3′ end of the guide strand because it interacts with the PAZ domain of the AGO2 protein.[16–19] It is expected that

covering the 3′ end of the guide strand destabilizes the interaction between siRNA and the Ago2 protein.

To our knowledge, this is the first report indicating that the target sequence preference of siRNAs can be modified by chemical bridging at the 2′ position of each ribose between the guide strand and the passenger strand, although the mechanisms by which the bridge attenuates silencing efficiency are unknown. As shown in the results, enhanced gene silencing was not observed with mRNA-based ESB RNAs, and reduced silencing efficiency was not demonstrated with antisense-based ESB RNAs, which may be important facts to resolve this mechanism. Indeed, three of the four target sequences of the ESB RNAs that exhibited reduced gene silencing were selected by mRNA-based target selection in which the 5′ end of the passenger strands are often GC rich and thermodynamically stable. It remains unclear how ESB RNA is activated in the RISC. Dallas et al. and other groups have proposed activation models for truncated shRNAs[30,31] in which the passenger strand is cleaved by Ago2 and maintains the 5′ half of the passenger strand tethered to the 3′ end of the guide strand via the loop structure, as reviewed by Herrera-Carrillo and Berkhout.[32] ESB RNAs may also be activated by a similar mechanism in which the 5′ half of the passenger strand is retained chemical bridging, despite cleavage of the passenger strand by Ago2. In this case, the remaining 5′ half of the passenger strand may reduce the accessibility of the guide strand to the target sequence because the 5′ end of the passenger strand designed by siRNA design tools is often GC rich and further stabilized by chemical bridging. In contrast, three of five target sequences of the ESB RNAs that showed enhanced gene silencing were selected by antisense-based target selection, in which the 3′ end of the guide strands are often AU rich to promote weaker hybridization, whereas the 5′ end of the guide strands tend to be GC rich and thermodynamically stable. Because covalent cross-linking locks hybridization around the 3′ end of the guide strand, it may simply be the result of an inversion of strand bias by stabilizing the 3′ end of the guide strand or steric hindrance during the interaction between the passenger strand and the RISC. It is also possible that chemical bridging affects the interaction between the ESB RNA and the proteins, such as Dicer and the double-stranded RNA-binding proteins, contributing to the guide strand selection.[14] Indeed, chemical bridging may inhibit protein function. We have tried to demonstrate RISC incorporation of ESB RNA by Ago2-immunoprecipitation and RT-PCR but could detect only a small signal due to the ESB RNA (data not shown), possibly owing to the inhibition of reverse transcription of the guide strand. The results shown in this article and in the patent for ESB RNA[33] have demonstrated that the structural factors essential for ESB RNA activity are quite similar to siRNA, but it is necessary to develop detection and quantification methods for ESB RNA to reveal the mechanism of action. In addition, to reveal factors associating with ESB RNA, further studies using cells lacking genes involved in RNAi pathways, such as Ago2, will be required.

We demonstrated that ESB RNA could strongly suppress the expression of the *EML4-ALK* fusion gene, whereas ordinary siRNA could not. Although *EML4-ALK* is just an example evaluated in a reporter system, the result clearly demonstrated that ESB RNA silenced the expression of both *EML4-ALK* fusion transcripts. It can be difficult for siRNAs to suppress target gene expression when the targetable sequences are limited, such as fusion genes, point mutations, or interspecies consensus sequences. We demonstrated that ESB RNAs exhibit a unique target preference that is somewhat different from siRNAs. In particular, ESB RNAs are highly efficient at silencing targets that are not suppressed by siRNAs, as shown in Figures 3 and 4. Therefore, ESB RNAs will complement siRNA-based gene silencing studies and expand the range of applications for RNAi technology.

MATERIALS AND METHODS

Target site selection and design of siRNAs and ESB RNAs

The sequences of the human NIMA related kinase 6 (*NEK6*) mRNA, hypoxanthine phosphoribosyltransferase 1 (*HPRT1*) mRNA, and glyceraldehyde-3-phosphate dehydrogenase (*GAPDH*) mRNA were obtained from GenBank (GenBank: NM_014397, NM_000194, and NM_002046, respectively). The target site of *NEK6* mRNA shown in Figures 1 and 2 was selected from a disclosed patent involving *NEK6*.[34] The sequences considered ineffective as siRNA targets shown in Figure 3B were selected using the siRNA design tool siDirect[25] (http://sidirect2.rnai.jp/) by applying the complementary (antisense) sequence to human *NEK6* mRNA. The target site of *HPRT1* was selected based on a previous report.[35,36] The target sites for *GAPDH* mRNA were selected based on an off-target prediction. The off-targets for each sequence were predicted using the off-target prediction tool in siSPOTR[24] (https://sispotr.icts.uiowa.edu/sispotr/tools/lookup/evaluate.html). The target sites were arbitrarily selected from sequences with a predicted off-target score of less than 100 (Table S1). The selected sequences were checked against the target site list obtained using siDirect to determine whether the *GAPDH* target sites that we identified were selected when the mRNA or its antisense sequence was applied. The mRNA sequences of the *EML4-ALK* variants 3a and 3b were obtained from GenBank (GenBank: AB374361 and AB374362, respectively). We selected three target sites as the junction located around the center of the target sites as shown in Figure 4. The siRNAs and ESB RNAs targeting the *EML4-ALK* transcripts were designed so the guide strands were fully complementary to the transcript variant 3a. All siRNAs were designed to be 19 bp with 2 nt overhangs at the 3′ ends of the guide and passenger strands. ESB RNAs with different stem lengths (16–22 bp) were designed as the 5′ ends of the guide strands to be at the same positions as the 5′ ends of the corresponding siRNA guide strands.

Chemical synthesis of siRNAs and ESB RNAs

All RNA oligonucleotides were synthesized using commercially available *tert*-butyldimethylsilyl (TBDMS) amidites and controlled-pore glass solid supports placed in columns that were attached to an ABI 3900 DNA/RNA synthesizer (Applied Biosystems, Waltham, MA, USA). The newly developed AEM amidites (Figure S1) were introduced at the bridging site of 2′-2′ ESB RNA, and 5′-amino-modifier C6 CEP or 3′-phthalimide-amino-modifier C6 CPG was introduced at the bridging site of the 3′-5′ ESB RNA. After completing solid-phase synthesis, the RNA oligonucleotides were purified by

preparative chromatography after removing the protecting groups by a conventional method. The purity of the RNA oligonucleotides was confirmed to be >90% pure by reverse-phase high-performance liquid chromatography (HPLC). To confirm that the target product was synthesized, the molecular weight of the resulting oligonucleotides was measured using LC coupled to an electrospray ionization quadrupole time-of-flight tandem mass spectrometer (LC-ESI-Q-TOF/MS; SYNAPT G2 MS, Waters Corporation, Milford, MA, USA).

To form a chemical bridge between the guide and passenger strands in 2′-2′ or 3′-5′ ESB RNAs, a 0.1 mM siRNA solution in 0.2 M phosphate buffer (pH 8.5) was shaken in the presence of 30 equivalents of bis(sulfosuccinimidyl)suberate disodium salt (Dojindo, Kumamoto, Japan) at room temperature for 4 h. Finally, the ESB RNAs were purified from the reaction mixture by reverse-phase HPLC.

Plasmid construction

To construct luciferase reporter vectors to measure guide strand-derived silencing activity, the oligonucleotides complementary to the passenger strand of the siRNAs or ESB RNAs were inserted into the *Xho* I-*Not* I site of the multiple cloning site of the psiCHECK-2 vector (Promega, Madison, WI, USA). The inserted target sequences for the human *HEK6* and *HPRT1* were 5′-GGA GAA GAG ATT CAT CTT ATC TC-3′ and 5′-GGA ATT TCA AAT CCA ACA AAG TC-3′, respectively. To determine the silencing efficiencies of the ESB RNAs against the *EML4-ALK* transcript variants separately, the target sequences of the *EML4-ALK* variant 3a or 3b were also inserted into the *Xho* I-*Not* I site of the multiple cloning site of the psiCHECK-2 vector. The inserted target sequences were 5′-TAA AGA TGT CAT CAT CAA CCA AGT GTA CCG CCG GAA GCA CCA GGA G-3′ for variant 3a and 5′-AAC TCG CGA AAA AAA CAG CCA AGT GTA CCG CCG GAA GCA CCA GGA G-3′ for variant 3b.

Cell culture and transfection

H1299 cells (ATCC, Manassas, VA, USA) and Dicer-deficient H1299 cells (kindly gifted from Prof. Masahiko Kuroda) were grown in RPMI-1640 medium supplemented with 10% heat-inactivated fetal bovine serum (JRH Biosciences, Lenexa, KS, USA). To measure the guide strand activity by qRT-PCR, the siRNAs or ESB RNAs were introduced into H1299 cells by a reverse transfection method. H1299 cells were seeded at 5×10^4 cells per well in 24-well plates with a mixture of siRNA or ESB RNA and the transfection reagent Lipofectamine RNAiMAX (Life Technologies, Carlsbad, CA, USA) according to the manufacturer's instructions.

HCT116 cells (RIKEN BRC, Tsukuba, Japan) were grown in DMEM medium (Sigma Aldrich, St. Louis, MO, USA) supplemented with 10% heat-inactivated fetal bovine serum (JRH Biosciences). To measure passenger strand activity in the luciferase assay, HCT116 cells were transfected with the luciferase expression vectors using a forward transfection method prior to the reverse transfection of the siRNAs or ESB RNAs. The cells were seeded at 2.5×10^5 cells per well in 6-well plates or 1×10^6 cells per 100 mm dish and cultured overnight. The next day, 500 ng/well or 2 μg/dish of the luciferase expression vectors were transfected into HCT116 cells using Lipofectamine 2000 (Life Technologies) according to the manufacturer's instructions. The cells transfected with the luciferase vectors were harvested 24 h after transfection and used for reverse transfection of siRNAs or ESB RNAs. The HCT116 cells transfected with the luciferase vectors were reseeded at 1×10^4 cells per well in 96-well plates with a mixture of siRNA or ESB RNA and the Lipofectamine RNAiMAX transfection reagent according to the manufacturer's instructions.

qRT-PCR

Total RNA was extracted using the RNeasy Mini kit (Qiagen, Hilden, Germany) followed by reverse transcription. qPCR using the PrimeScript One Step RT-PCR kit (TaKaRa, Kusatsu, Japan) was performed according to the manufacturer's instructions. The primers used were as follows: 5′-GGA GTT CCA ACA ACC TCT GC-3′ and 5′-GAG CCA CTG TCT TCC TGT CC-3′ for *NEK6*; 5′-GAA AAG GAC CCC ACG AAG TGT-3′ and 5′-AGT CAA GGG CAT ATC CTA CAA CA-3′ for *HPRT1*; and 5′-ATG GGG AAG GTG AAG GTC G-3′ and 5′-GGG TCA TTG ATG GCA ACA ATA TC-3′ for *GAPDH*. The qRT-PCR was carried out using the LightCycler 480 System II (Roche, Basel, Switzerland), and the resulting Cp values were used to calculate the relative expression levels of the target genes by the ΔΔCt method. The expression levels were defined as the ratio of the expression of the internal control genes. Thus, *NEK6* and *HPRT1* were normalized to *GAPDH*, and *GAPDH* was normalized to *HPRT1*.

Luciferase assay

The HCT116 cells transfected with luciferase vectors were lysed 24 h after transfection of siRNAs or ESB RNAs. Luciferase activity was measured with the Dual-Glo Luciferase Assay System (Promega) using ARVO X2 (PerkinElmer, Waltham, MA, USA) and defined as the ratio of the reporter *Renilla* luciferase activity to the internal control firefly luciferase activity.

Statistical analysis

Data are presented as the mean ± SD. Statistical differences between the two groups were evaluated using a two-tailed Student's t test assuming equal variance. $p < 0.05$ was considered statistically significant.

DATA AVAILABILITY STATEMENT

Qualified researchers can request access to the data supporting the findings of this study from Bonac Corporation by contacting atsushi.shibata@bonac.co.jp.

SUPPLEMENTAL INFORMATION

Supplemental information can be found online at https://doi.org/10.1016/j.omtn.2023.04.013.

ACKNOWLEDGMENTS

We would like to dedicate this paper to the late Dr. Yutaka Eguchi, who gave us the opportunity to start this project. We thank Dr. Wataru Toriumi from the Fukuoka Center for Disease Control and Prevention for an insightful discussion and support for publication. We also thank Mr. Hirotake Hayashi from the Bonac Corporation for great encouragement and Prof. Masahiko Kuroda from the Tokyo Medical University for the kind gift of the Dicer-deficient cells. The authors would like to thank Enago (www.enago.jp) for the English language review.

AUTHOR CONTRIBUTIONS

The AEM amidite was conceived by T.O. and developed by T.A. T.A., C.E., and E.A. synthesized ESB RNAs. H.S. designed the reporter vectors and carried out luciferase assays. H.S. and Y.I. performed qRT-PCR analyses. The study was conceived by A.S. and supervised by T.O. and A.S. The manuscript was written by A.S., and it was reviewed and edited by H.S., E.A., and T.O. All authors read and approved the manuscript.

DECLARATION OF INTERESTS

All authors are past or current employees of Bonac Corporation (Kurume, Japan), who funded this work and have a patent related to this work: WO/2022/045224, Novel nucleic acid molecule inhibiting the expression of a target gene.

REFERENCES

1. Fire, A., Xu, S., Montgomery, M.K., Kostas, S.A., Driver, S.E., and Mello, C.C. (1998). Potent and specific genetic interference by double-stranded RNA in *Caenorhabditis elegans*. Nature *391*, 806–811.
2. Napoli, C., Lemieux, C., and Jorgensen, R. (1990). Introduction of a chimeric chalcone synthase gene into petunia results in reversible co-suppression of homologous genes in trans. Plant Cell *2*, 279–289.
3. Elbashir, S.M., Harborth, J., Lendeckel, W., Yalcin, A., Weber, K., and Tuschl, T. (2001). Duplexes of 21-nucleotide RNAs mediate RNA interference in cultured mammalian cells. Nature *411*, 494–498.
4. Brummelkamp, T.R., Bernards, R., and Agami, R. (2002). A system for stable expression of short interfering RNAs in mammalian cells. Science *296*, 550–553.
5. Nikam, R.R., and Gore, K.R. (2018). Journey of siRNA: clinical developments and targeted delivery. Nucleic Acid Ther. *28*, 209–224.
6. Setten, R.L., Rossi, J.J., and Han, S.P. (2019). The current state and future directions of RNAi-based therapeutics. Nat. Rev. Drug Discov. *18*, 421–446.
7. Zhang, M.M., Bahal, R., Rasmussen, T.P., Manautou, J.E., and Zhong, X.B. (2021). The growth of siRNA-based therapeutics: updated clinical studies. Biochem. Pharmacol. *189*, 114432.
8. Schwarz, D.S., Hutvágner, G., Du, T., Xu, Z., Aronin, N., and Zamore, P.D. (2003). Asymmetry in the assembly of the RNAi enzyme complex. Cell *115*, 199–208.
9. Khvorova, A., Reynolds, A., and Jayasena, S.D. (2003). Functional siRNAs and miRNAs exhibit strand bias. Cell *115*, 209–216.
10. Reynolds, A., Leake, D., Boese, Q., Scaringe, S., Marshall, W.S., and Khvorova, A. (2004). Rational siRNA design for RNA interference. Nat. Biotechnol. *22*, 326–330.
11. Ui-Tei, K., Naito, Y., Takahashi, F., Haraguchi, T., Ohki-Hamazaki, H., Juni, A., Ueda, R., and Saigo, K. (2004). Guidelines for the selection of highly effective siRNA sequences for mammalian and chick RNA interference. Nucleic Acids Res. *32*, 936–948.
12. Amarzguioui, M., and Prydz, H. (2004). An algorithm for selection of functional siRNA sequences. Biochem. Biophys. Res. Commun. *316*, 1050–1058.
13. Wang, B., Li, S., Qi, H.H., Chowdhury, D., Shi, Y., and Novina, C.D. (2009). Distinct passenger strand and mRNA cleavage activities of human Argonaute proteins. Nat. Struct. Mol. Biol. *16*, 1259–1266.
14. Noland, C.L., and Doudna, J.A. (2013). Multiple sensors ensure guide strand selection in human RNAi pathways. RNA *19*, 639–648.
15. Lisowiec-Wąchnicka, J., Bartyś, N., and Pasternak, A. (2019). A systematic study on the influence of thermodynamic asymmetry of 5′-ends of siRNA duplexes in relation to their silencing potency. Sci. Rep. *9*, 2477.
16. Wang, Y., Sheng, G., Juranek, S., Tuschl, T., and Patel, D.J. (2008). Structure of the guide-strand-containing argonaute silencing complex. Nature *456*, 209–213.
17. Frank, F., Sonenberg, N., and Nagar, B. (2010). Structural basis for 5′-nucleotide base-specific recognition of guide RNA by human AGO2. Nature *465*, 818–822.
18. Boland, A., Tritschler, F., Heimstädt, S., Izaurralde, E., and Weichenrieder, O. (2010). Crystal structure and ligand binding of the MID domain of a eukaryotic Argonaute protein. EMBO Rep. *11*, 522–527.
19. Yoda, M., Kawamata, T., Paroo, Z., Ye, X., Iwasaki, S., Liu, Q., and Tomari, Y. (2010). ATP-dependent human RISC assembly pathways. Nat. Struct. Mol. Biol. *17*, 17–23.
20. Siolas, D., Lerner, C., Burchard, J., Ge, W., Linsley, P.S., Paddison, P.J., Hannon, G.J., and Cleary, M.A. (2005). Synthetic shRNAs as potent RNAi triggers. Nat. Biotechnol. *23*, 227–231.
21. Ge, Q., Ilves, H., Dallas, A., Kumar, P., Shorenstein, J., Kazakov, S.A., and Johnston, B.H. (2010). Minimal-length short hairpin RNAs: the relationship of structure and RNAi activity. RNA *16*, 106–117.
22. Liu, Y.P., Schopman, N.C.T., and Berkhout, B. (2013). Dicer-independent processing of short hairpin RNAs. Nucleic Acids Res. *41*, 3723–3733.
23. Kaadt, E., Alsing, S., Cecchi, C.R., Damgaard, C.K., Corydon, T.J., and Aagaard, L. (2019). Efficient knockdown and lack of passenger strand activity by Dicer-independent shRNAs expressed from Pol II-driven microRNA scaffolds. Mol. Ther. Nucleic Acids *14*, 318–328.
24. Boudreau, R.L., Spengler, R.M., Hylock, R.H., Kusenda, B.J., Davis, H.A., Eichmann, D.A., and Davidson, B.L. (2013). siSPOTR: a tool for designing highly specific and potent siRNAs for human and mouse. Nucleic Acid Res. *41*, e9.
25. Naito, Y., Yoshimura, J., Morishita, S., and Ui-Tei, K. (2009). siDirect 2.0: updated software for designing functional siRNA with reduced seed-dependent off-target effect. BMC Bioinformatics *10*, 392.
26. Choi, Y.L., Takeuchi, K., Soda, M., Inamura, K., Togashi, Y., Hatano, S., Enomoto, M., Hamada, T., Haruta, H., Watanabe, H., et al. (2008). Identification of novel isoforms of the *EML4-ALK* transforming gene in non-small cell lung cancer. Cancer Res. *68*, 4971–4976.
27. Sasaki, T., Rodig, S.J., Chirieac, L.R., and Jänne, P.A. (2010). The biology and treatment of *EML4-ALK* non-small cell lung cancer. Eur. J. Cancer *46*, 1773–1780.
28. Shinmura, K., Kageyama, S., Igarashi, H., Kamo, T., Mochizuki, T., Suzuki, K., Tanahashi, M., Niwa, H., Ogawa, H., and Sugimura, H. (2010). EML4-ALK fusion transcripts in immunohistochemically ALK-positive non-small cell lung carcinomas. Exp. Ther. Med. *1*, 271–275.
29. Chen, P.Y., Weinmann, L., Gaidatzis, D., Pei, Y., Zavolan, M., Tuschl, T., and Meister, G. (2008). Strand-specific 5′-O-methylation of siRNA duplexes controls guide strand selection and targeting specificity. RNA *14*, 263–274.
30. Dallas, A., Ilves, H., Ge, Q., Kumar, P., Shorenstein, J., Kazakov, S.A., Cuellar, T.L., McManus, M.T., Behlke, M.A., and Johnston, B.H. (2012). Right- and left-loop short shRNAs have distinct and unusual mechanisms of gene silencing. Nucleic Acids Res. *40*, 9255–9271.
31. Sun, G., Yeh, S.Y., Yuan, C.W.Y., Chiu, M.J.Y., Yung, B.S.H., and Yen, Y. (2015). Molecular properties, functional mechanisms, and applications of sliced siRNA. Mol. Ther. Nucleic Acids *4*, e221.
32. Herrera-Carrillo, E., and Berkhout, B. (2017). Dicer-independent processing of small RNA duplexes: mechanistic insights and applications. Nucleic Acids Res. *45*, 10369–10379.

33. Shibata, A., Ohgi, T., Abe, T., Emura, C., Aoki, E., Shirohzu, H., Iwakami, Y., Ramirez, M.A., and Naito, K. (2022). Novel Nucleic Acid Molecule Inhibiting Expression of Target Gene. Patent No. WO/2022/045224.

34. Nakao, K., Ishiyama, J., Ichikawa, W., Masui, A., Akasaka, Y., and Honda, A. (2020). Therapeutic Agent for Fibrosis. Patent No. WO/2020/152869.

35. Andaloussi, S.E.L., Lehto, T., Mäger, I., Rosenthal-Aizman, K., Oprea, I.I., Simonson, O.E., Sork, H., Ezzat, K., Copolovici, D.M., Kurrikoff, K., et al. (2011). Design of a peptide-based vector, PepFect6, for efficient delivery of siRNA in cell culture and systemically in vivo. Nucleic Acids Res. *39*, 3972–3987.

36. Collingwood, M.A., Rose, S.D., Huang, L., Hillier, C., Amarzguioui, M., Wiiger, M.T., Soifer, H.S., Rossi, J.J., and Behlke, M.A. (2008). Chemical modification patterns compatible with high potency dicer-substrate small interfering RNAs. Oligonucleotides *18*, 187–200.